

Climate change projections of sea level extremes along the California coast

Daniel R. Cayan · Peter D. Bromirski ·
Katharine Hayhoe · Mary Tyree ·
Michael D. Dettinger · Reinhard E. Flick

Received: 2 August 2006 / Accepted: 5 October 2007
© Springer Science + Business Media B.V. 2007

Abstract California's coastal observations and global model projections indicate that California's open coast and estuaries will experience rising sea levels over the next century. During the last several decades, the upward historical trends, quantified from a small set of California tide gages, have been approximately 20 cm/century, quite similar to that estimated for global mean sea level. In the next several decades, warming produced by climate model simulations indicates that sea level rise (SLR) could substantially exceed the rate experienced during modern human development along the California coast and estuaries. A range of future SLR is estimated from a set of climate simulations governed by lower (B1), middle–upper (A2), and higher (A1fi) GHG emission scenarios. Projecting SLR from the ocean warming in GCMs, observational evidence of SLR, and separate calculations using a simple climate model yields a range of potential sea level increases, from 11 to 72 cm, by the 2070–2099 period. The combination of predicted astronomical tides with projected weather forcing, El Niño related variability, and secular SLR, gives a series of hourly sea level projections for 2005–2100. Gradual sea level rise progressively worsens the impacts of high tides, surge and waves resulting from storms, and also freshwater floods from Sierra and coastal mountain catchments. The occurrence of extreme sea levels is pronounced when these factors coincide. The frequency and magnitude of extreme events, relative to current levels, follows a sharply escalating pattern as the magnitude of future sea level rise increases.

D. R. Cayan (✉) · P. D. Bromirski · M. Tyree · M. D. Dettinger · R. E. Flick
Scripps Institution of Oceanography, University of California, La Jolla, CA, USA
e-mail: dcayan@ucsd.edu

D. R. Cayan · M. D. Dettinger
Water Resources Division, U. S. Geological Survey, La Jolla, CA, USA

K. Hayhoe
Department of Geosciences, Texas Tech University, Lubbock, TX, USA

R. E. Flick
California Department of Boating and Waterways, La Jolla, CA, USA

1 Introduction

California has about 1,800 km of coastline, numerous estuaries including the San Francisco Bay and Delta, wetlands, and coastal aquifers. These are susceptible to harmful effects if sea level rises too much or too fast.

For at least the past 20,000 years, sea level has been rising at various rates as a result of the last and ongoing episode of global warming and associated glacial and icecap melting and retreat. (Fairbanks 1989). During the most rapid period of rise from about 18,000 to about 5,000 years ago, sea level rose nearly 120 m (almost 400 ft), or an average of about 100 cm/century. Sea level is estimated to have risen at an average rate of about 5 cm/century during the past 6,000 years, and at an average rate of 1 to 2 cm/century during the past 3,000 years (Church et al. 2001). Wave cut platforms attest to these rates along California's coastline.

During the twentieth century, from a collection of tide gages, global sea level rose an estimated 1.8 mm/year (Church et al. 2001), and during the recent few decades, global sea level rise appears to have risen faster, in excess of 2.2 mm/year (Cazenave and Nerem 2004; Holgate and Woodworth 2004; Church and White 2006). Identifying sources of the global rise has been a conundrum, in that estimates of the two predominant sources, steric increases in ocean volume due to thermal expansion and eustatic increases due to melting of ground-based ice only accounts for about half of this estimated increase (Munk 2002; Cazenave and Nerem 2004), although a recent reanalysis (Mitrovica et al. 2006) of ancient eclipse, astronomic and geodetic data yields a result that is more consistent with recent observationally-based sea level rise estimates, and suggests that ice melt of approximately 1 mm/year has contributed. Tide gauge records in California and other west coast United States locations that are tectonically stable (Fig. 1) show corresponding rises (although the correspondence may be chance). Sea-level rise (SLR) along the West Coast has been more or less continuous during the twentieth century, but has been marked by considerable interannual and decadal variability (Bromirski et al. 2003). Interestingly, the records in Fig. 1 do not indicate recent increases in the rates of SLR along the California Coast, but rather have been relatively flat since about 1983. This is because mean coastal sea levels depend on regional dynamical adjustments, and thus can be significantly different from the global mean (Cabanes et al. 2001). However, viewed over the longer term, rising sea levels have had a strong coastal influence along the entire California coast. The occurrence of extremes has increased markedly (Table 1), e.g., levels above the 99.99th percentile has increased at San Francisco (by 20-fold since 1915) and at La Jolla (by 30-fold since 1933). As sea level continues to rise, these extremes will become even more common. In this paper, we evaluate the possible evolution and properties of twenty-first century sea-level extremes, consistent with climate-change projections described elsewhere in this volume.

2 Short-period variations of California sea level

The long term trends in sea level discussed above establish the base level upon which an envelope of short-term sea-level fluctuations operates, which together yield the observed sea level.

Although mean sea level (MSL) rise often gets much of the attention when sea level height (SLH) variability is considered, tidal, storm surge, and longer period SLH variability on time scales up to several years are superimposed upon MSL and produce great impacts along the West Coast of North America on an annual basis. Storm surge events are relatively local, typically spanning periods of a few days, and dominate non-tidal short

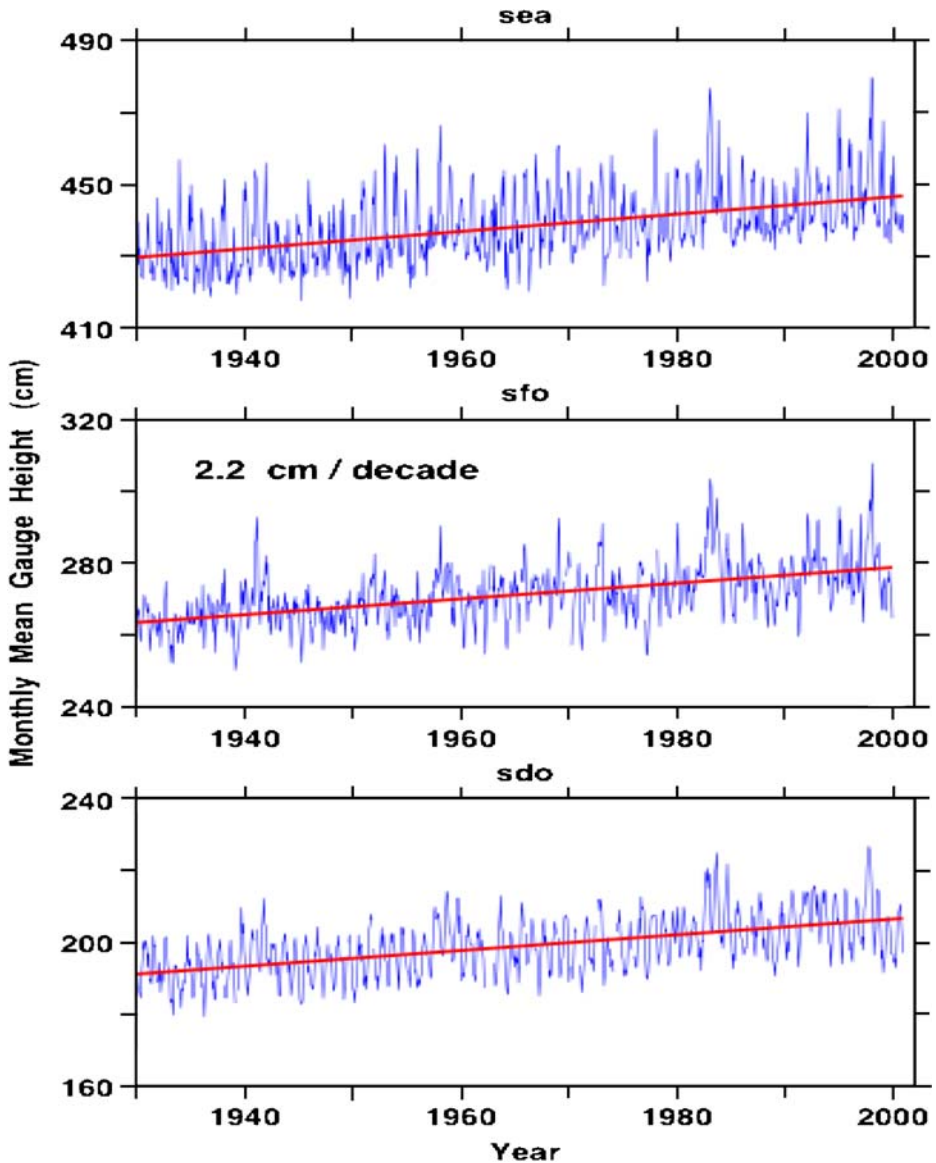


Fig. 1 Observed monthly mean sea level (cm) from Seattle, San Francisco, San Diego tide gauges. Least squares trends (*red lines*) have similar slopes, and represent the regional sea level upon which shorter duration SLH fluctuations are superimposed

period SLH fluctuations, while monthly-to-interannual SLH fluctuations associated with El Niño/Southern Oscillation (ENSO) contribute the dominant part of sea level variability at seasonal to interannual time scales. The greatest coastal impacts occur when elevated storm surge coincides with high tides near peaks of longer period SLH fluctuations, all of which are superimposed on MSL. Most of the “spread” in the distribution of sea levels is caused by astronomical tides, i.e. the regular changes of ocean water levels caused by the gravitational forces of the moon and sun. Tides are almost always the largest components of

daily sea level fluctuations, with the California open coast tide range of up to about 3 m, trough to peak (Table 1). Tides are the only component of sea-level variability that are accurately predictable.

The most important tidal time scales on the California coast are semidiurnal, diurnal, semi-monthly, semiannual and 4.4 years. California's tide regime is distinctly different from the semi-diurnal conditions that dominate the east coast of the United States. On the California coast, tides are mixed, periodically having nearly equal semi-daily and daily components (Zetler and Flick 1985). The monthly tidal changes are dominated by the spring-neap cycle, with two periods with large tidal ranges (springs) near the times of full and new moon, and two periods with lower ranges (neaps) near times of the quarter moons. One spring tide range per month is usually higher than the other, a consequence of the moon's distance and declination. As a result of lunar and solar declination effects, highest monthly tides in the winter and summer months are higher than those in the spring and fall, with their respective differences ranging up to about 0.5 m. Furthermore, the extreme monthly higher-high tides in the winter tend to occur in the morning, sometimes quite early (Flick 2000). On the California coast, the distinct 4.4-year cycle results in peak monthly tides about 0.15 m higher, compared with years in between. This cycle peaked in 1982–1983, 1986–1987, 1990–1991, 1995–1996, and 1999–2000, etc.

Other less predictable fluctuations also contribute to local sea level changes, including storm surges, large scale changes in water temperature and wind forcing, and climate related fluctuations (Flick 1998). Storm surge is that portion of the local, instantaneous sea level elevation that exceeds the predicted tide and which is attributable to the effects of low barometric pressure and high wind associated with storms. Storm surge along the California coast, excluding the effect of waves, rarely exceeds 0.7 m in amplitude. However, wave induced surge on a beach, depending on breaker height, can reach 1.5 m or more. During El Niños, large scale oceanic and atmospheric mechanisms often elevate sea level along the West Coast (Chelton and Davis 1982; Flick 1998; Seymour et al. 1984; Seymour, 1998; Storlazzi and Griggs 1998; Bromirski et al. 2003), yielding non-tide sea-level anomalies with amplitudes of 10–20 cm that may persist for several months.

3 Projections of global sea level rise

Over the next few hundred years, global sea level is expected to rise because, at present, the earth's radiation budget is out of balance (Hansen 2005) and the earth, especially the

Table 1 Observed high sea level occurrences from San Francisco and La Jolla tide gauge records

	San Fran			La Jolla		
	# > 99.99th	Max s.l. (m)	No. obs	# > 99.99th	Max s.l. (m)	No. obs.
1915–1933	1	1.43427	157,798			
1933–1951	5	1.44627	157,776	0	1.31815	148,375
1951–1969	7	1.45627	157,137	3	1.47315	144,392
1969–1987	36	1.80027	155,396	29	1.52515	145,562
1987–2004	29	1.68027	149,016	24	1.54615	148,320

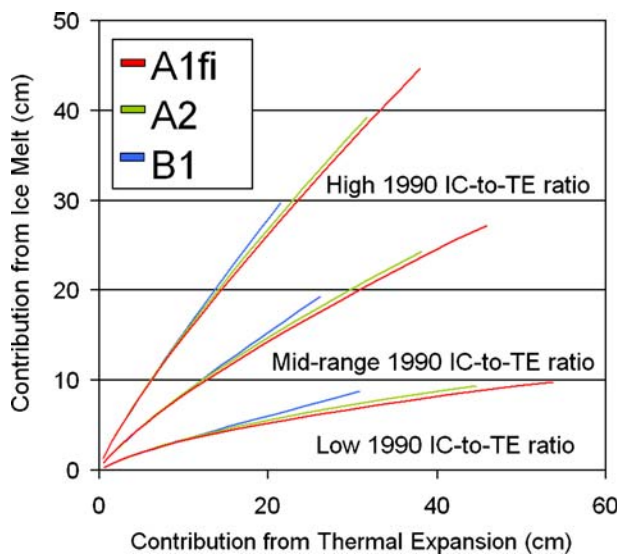
Number of exceedances above 99.99th percentile thresholds from 1933 to 2004 hourly observations. Maximum values are relative to mean sea level.

San Francisco 99.99th percentile=141 cm, La Jolla (Scripps Pier) 99.99th percentile=141.2 cm

oceans, is still heating (Wigley 2005; Meehl et al. 2005) Also, in the foreseeable future, projected increases in greenhouse gases and associated increases in temperature are expected to further warm the oceans (Church et al. 2001). SLR of several cm is likely from thermal expansion of sea water, but eventually, sea level could rise several meters from melting of continental ground-based ice, especially in Greenland and Antarctica (Alley et al. 2005). Although it is likely that there will be regional differences in coastal sea levels (Mitrovica et al. 2001; Cabanes et al. 2001), because the historical rate of mean sea level increase at California tide gages is quite similar to the estimated global SLR, the hypothesis used here is that future SLR in California can be approximated by future SLR estimated for the global ocean.

Projected ranges in SLR due to thermal expansion (TE) are a natural outgrowth of recent projections of warming over the next century, and are available from climate simulations of the IPCC SRES A2 and B1 greenhouse-gas (GHG) emissions scenarios. However, SLR due to land-ice melt (IM) is not yet a part of the latest projections. Because ice melt is an important component of global SLR (Church et al. 2001, Cazenave and Nerem 2004), an accounting of the land-ice melt contributions is necessary to estimate overall SLR. For a guideline of likely or possible sea level rise in California during the next century, we use the TE component from the GCM’s together with the MAGICC “simple climate model” (Hulme et al. 1995; Wigley 2005) to derive sea level changes over the 100 year projection. The starting point of this model exercise uses as an initial value the relative contributions of TE and IM. The model then calculates, stepping forward in time, the amount of SLR, including its TE and IM components. Because of the uncertainty in the relative fraction of these two components, the MAGICC calculation is repeated using three (high, medium, and low) estimates of IM vs. TE, as shown in Fig. 2. SLR projections for the A1fi scenario (high greenhouse gas emissions) were not available from the climate models analyzed in the present study. Therefore, A1fi values of TE were estimated from A1fi simulations by previous models, based on the differences between A2 projections from those previous models and the current A2 projections. The IM contribution was then estimated by the approach described above.

Fig. 2 MAGICC-simulated relationship between the relative contributions of ice melt and thermal expansion to global sea level rise estimates over the next century, corresponding to the range of historical ratios derived from observational and modeling studies



A superposition of the associated SLR estimates corresponding to the different GCM and emission scenario simulations produces an envelope of possible sea level rise from 2000–2100, shown in Fig. 3. By mid-century (2035–2064), projections of global SLR range from ~6–32 cm above 1990 levels, with no discernable inter-scenario differences, as shown in Fig. 3 and Table 2. By end-of-century (2070–2100), however, SLR projections range from 10–54 cm under B1, to 14–61 cm under A2, and 17–72 cm under A1fi.

4 A model of hourly sea levels

To investigate the possible influence of SLR (and other climate changes) on the future statistics of extreme sea levels, a model of hourly sea level variations at three California coastal tide gage stations (Crescent City, San Francisco, and La Jolla) was developed. The model includes astronomical tides, weather effects, an El Niño influence, and secular sea level rise, as described in (a–d below). Although the astronomical tide component is based on a realistic tide prediction carried out over actual time during the twenty-first century, the other factors are hypothetical, drawn from climate model projections.

- (a) Astronomical tides are predicted with good precision based on known tidal constituents (Zetler and Flick 1985; Munk and Cartwright 1966) using a typical tidal prediction program developed by Munk (personal communication) and his co-workers at Scripps Institution of Oceanography. The standard tidal harmonic information published by NOAA on their website was used for each location. This consists of between about 20 and 30 constituents with amplitude and phase values derived from past observations. Corrections for apparent secular increases in the amplitude of the tide were not included (Flick et al. 2003).
- (b) Sea level fluctuations due to barometric (sea level pressure, SLP) and wind stress fluctuations were modeled using linear regression equations relating historical non-tidal sea level residuals (Bromirski et al. 2003) to local SLP and offshore wind stresses from the NCAR/NCEP Reanalysis dataset, 1950–2004 (Kalnay et al. 1996). The

Fig. 3 Projected sea level rise from climate model estimates for three GHG emissions scenarios, A1fi (high emissions), A2 (medium-high emissions) and B1 (low emissions)

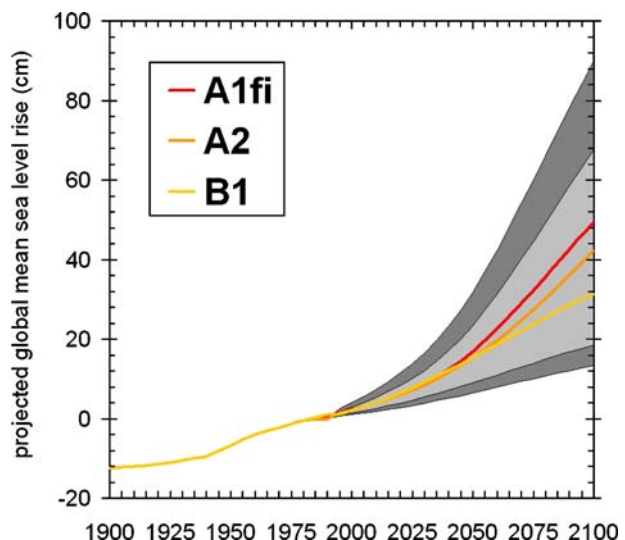


Table 2 Projected global sea level rise, in cm, relative to historical mean sea level, for the SRES A1fi, A2 and B1 scenarios as estimated by the latest AOGCM simulations combined with MAGICC projections for the ice melt component and the A1fi scenario

	B1			A2			A1fi		
	<i>Lo</i>	<i>Med</i>	<i>Hi</i>	<i>Lo</i>	<i>Med</i>	<i>Hi</i>	<i>Lo</i>	<i>Med</i>	<i>Hi</i>
1971–2000	−0.5	−0.2	0.4	−0.5	−0.2	0.3	−0.5	−0.1	0.4
2035–2064	6.0	14.9	31.1	6.3	15.1	28.8	7.1	16.9	32.2
2070–2099	10.9	26.4	53.9	14.2	32.8	60.5	16.8	38.7	71.6

greatest influence on short period non-tide sea level variability is that from inverse barometer effects, with wind stress contributing only incrementally. Time series of twenty-first century SLP and wind stresses were extracted from each of four atmosphere–ocean general circulation model (GCM) simulations: A2 and B1 scenarios simulated by the NOAA Geophysical Fluid Dynamics Laboratory (GFDL) CM2.1 model (Delworth et al. 2006) and by the National Center for Atmospheric Research (NCAR) Parallel Climate Model (PCM) (Washington et al. 2000). (Because SLR projections from each of several simulations were similar, only results from the GFDL A2 simulation are shown here.) SLP simulated by the models has mean and variance that are in good agreement with SLP from the NCEP Reanalysis. The sea-level model was applied at hourly intervals in order to capture synoptic variability. But because the climate projections and Reanalysis were only available at daily, not hourly, intervals, additional disaggregation of the inputs was required. To synthesize hourly SLP, a day-long sequence of hourly SLP observed at airport weather stations was interjected around each simulated day's daily mean, with requirements that: (1) the mean daily SLP from the weather station was within 8 hPa of the projection's daily mean, and (2) the first hour of a given day's SLP matched the last hour of the preceding day's SLP within 4 hPa in order to retain a relatively realistic and smoothly varying SLP predictor. Hourly wind stress variations were generated using simple linear interpolation between the daily mean values from the GCM, centered at mid-day.

- (c) Monthly-to-interannual sea-level fluctuations associated with El Niño/Southern Oscillation (ENSO) contribute the dominant part of sea level variability at seasonal-interannual time scales. The ENSO component was incorporated using a simple regression equation relating monthly NINO 3.4 SSTs (averaged over 120°W–170°W, 5°S–5°N) to smoothed observed sea levels at California's tide stations. Assuming that the same relationships operate in the future, ENSO variability was extracted from the climate simulations as detrended NINO 3.4 SSTs, which were rescaled to match the standard deviation of the observed NINO 3.4 series for 1961–1990. In the GFDL CM2.1 simulations, this NINO 3.4 SST index was well correlated with another commonly used ENSO index, the Southern Oscillation Index; correlation coefficients were −0.65 for monthly data, September through February; and −0.82 for seasonal mean data from the GFDL CM2.1 2005–2099 A2 simulation. Using these projected NINO 3.4 values, the corresponding ENSO-induced sea-level fluctuations for California were projected using the historical regression relation. Because the ENSO and weather components were extracted from the same climate model sequences at known points in (future) time, the simultaneity of the ENSO, weather, and tidal contributions was ensured. Two other North Pacific climate indices, NP (Trenberth

and Hurrell 1994) and PNA (Wallace and Gutzler 1981), did not account for significant fractions of variance of the sea level anomaly at the three coastal stations, so they were not included as predictors.

- (d) Finally, mean SLR was obtained from Fig. 3. To cover the range of potential SLR, a set of linear rates from +10 to +80 cm per hundred years were added to the short term sea-level components.

Simulated sea level anomalies and resultant total sea level height is shown in Fig. 4 for a two month period during winter 2006 San Francisco. The variability of the simulated sea level anomaly series resembles that from the observed sea level anomaly. There is also good correspondence between the magnitude and temporal variations of the monthly average simulated sea level and that from historical observations, as shown in Fig. 5 for the 2000–2100 GFDL simulated series in comparison to 1900–2000 observed sea level from the San Francisco record. Other simulations constructed from the GFDL CM2.1 B1 emissions scenario and from PCM A2 and B1 emissions scenarios, produced quantitatively similar results as those for the GFDL CM2.1 A2 simulation, so they are not shown here.

The regression relations and correlations obtained from observed sea levels at Crescent City, San Francisco, and La Jolla are given in Table 3. The model replicates approximately 50% of the historical daily mean sea level height anomaly variance using three relatively simple weather inputs: SLP, zonal, and meridional wind stress components. The overall fraction of variance of the non-tidal sea level anomalies, not including the variability introduced by the long period trend, ranged from 68% at Crescent City to 45% at La Jolla, as shown in Table 3. These differences reflect a pattern of increasing magnitudes of storm activity (winds and barometric pressure fluctuations) and anomalous short period climate variability from lower to higher mid-latitudes along the west coast of North America. The variability in the linear model is of similar magnitude, but somewhat smaller than that in the observations, with model standard deviations ranging from 82% (Crescent City) to 66% (La Jolla) of those of the observed sea level daily non-tide anomalies. SLP provided the dominant fraction of the explained variance; only about 10% was explained by the wind stress components. A reasonable fraction of the monthly to interannual variability of sea level anomaly was explained by NINO 3.4, with approximately 5 cm of sea level per °C of NINO 3.4 SST anomaly, meaning that a significant, +2°C SST anomaly, El Niño will raise sea level at the coastal stations by about 10 cm.

5 Exploration of possible sea level extremes during the 21st Century

Climate change is likely to raise mean sea levels, which would lead to inundation of some low-lying areas and adversely affect coastal aquifers. However, some of the most serious impacts would result from the extreme sea levels associated with tides, winter storms, and other episodic events that would be superimposed upon the higher baseline sea level. Extreme high water levels (measured by any fixed threshold) will occur with increasing frequency (i.e., with shorter return period) as a result of higher mean sea level. Many California coastal areas are at risk from sea level extremes, especially in combination with winter storms (Flick 1998). During the 1997–1998 El Niño, very high seas and storm surge caused hundreds of millions of dollars in storm and flood damage in the San Francisco Bay area. Highways were flooded as six-foot waves splashed over waterfront bulkheads, and valuable coastal real estate was destroyed (Ryan et al. 2000).

The frequency of high sea level extremes also may be increased if storms become more frequent or severe as a result of climate change. Increases in the duration of high storm-

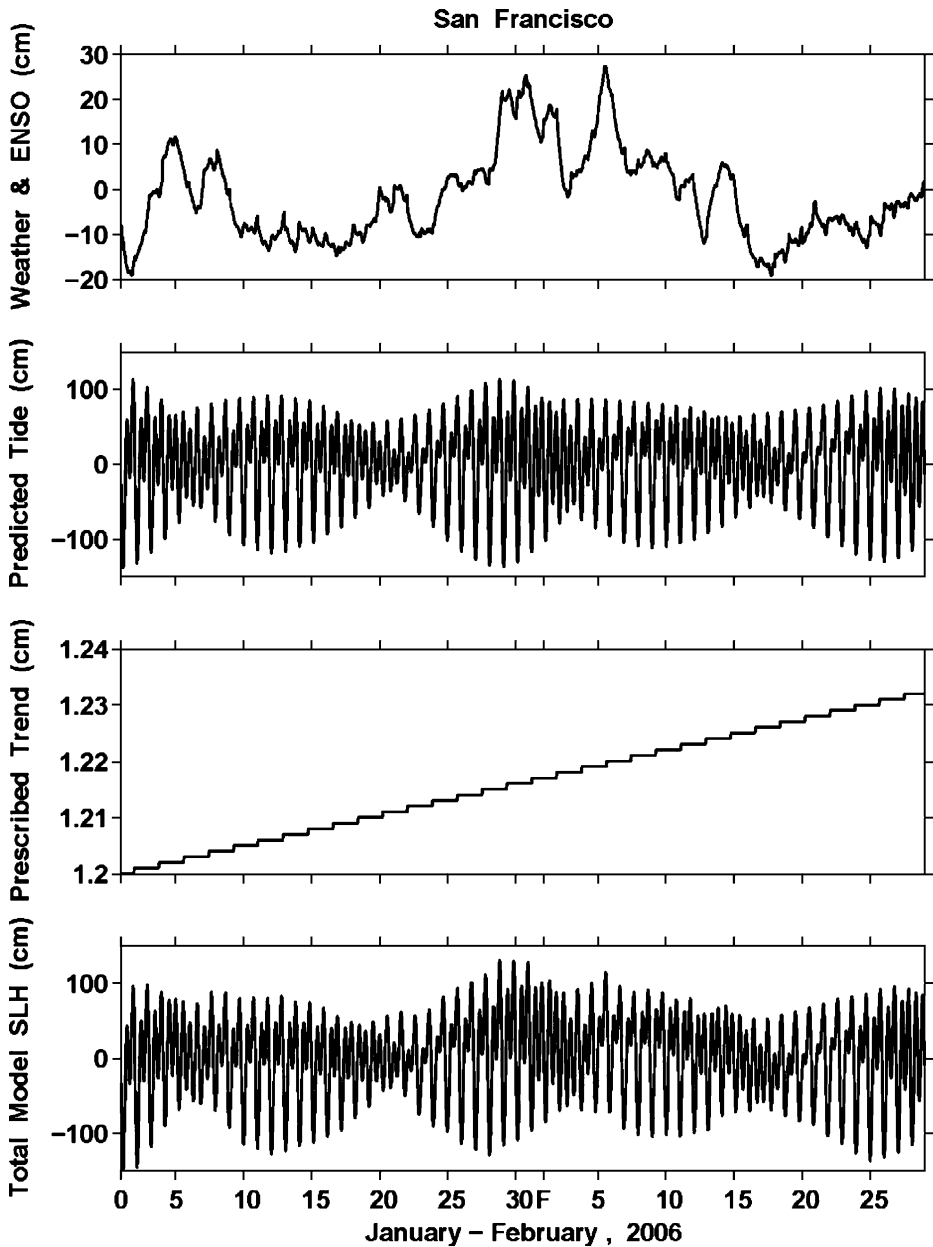


Fig. 4 Modeled sea levels include (*from top down*): non-tide, astronomical tide-prediction, and linear trend (20 cm/century), giving the total model sea level, January–February 2006 (*bottom*)

forced sea levels increases the likelihood that they will occur during high tides. The combination of severe winter storms with SLR and high tides would result in extreme sea levels that could expose the coast to severe flooding and erosion, damage to coastal structures and real estate, and salinity intrusion into delta areas and coastal aquifers.

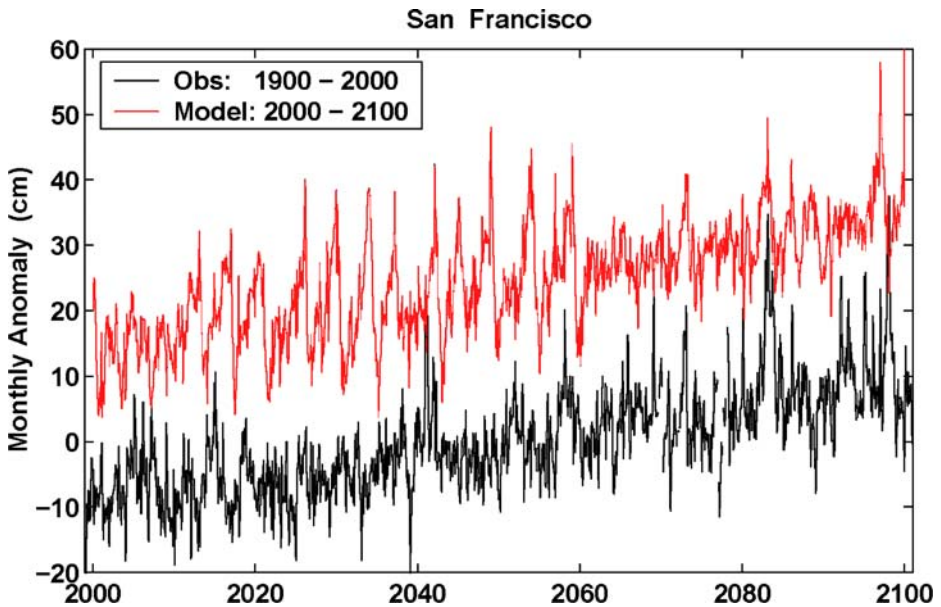


Fig. 5 Model projected (red) monthly San Francisco sea level anomalies from mean sea level, for 2000–2100 from GFDL A2 model input with linear trend amounting to 20 cm increase, 2000–2100. Observed (black) monthly sea level from San Francisco tide gage (1900–2100) is shown for comparison

Not surprisingly, then, projected sea level extremes, relative to the current sea level baseline, increase greatly as sea level rises. There is a marked increase of sea level extremes as sea level increases (a) over the twenty-first century, and (b) as the imposed SLR rate is increased from zero to 80 cm over the 100-year period. Table 4 describes how, at San Francisco, with 30 cm/century rate of rise, the occurrence of events above its historical (1960–1978) 99.99 percentile (141 cm above mean sea level) increases from just less than one hourly event in 1 year to about 1.3 events per year averaged over 2005–2034, to about seven events per year during 2035–2064, and to about 17 events per year in 2070–2099. If, instead, the rate of SLR is 60 cm/century, the incidence of hourly events exceeding the historical 99.99 percentile climbs to 4.6 per year during 2005–2034, to about 41 per year during 2035–2064, and to about 235 per year during 2070–2099. Similar increases in the

Table 3 Linear regression model of non-tide sea level residuals based on Reanalysis and Niño 3.4 input as predictors of daily sea level, 1950–2002

	Regression coefficients ^a				Goodness of fit			<i>R</i> non-tide s.l. vs. NINO 3.4 ^b
	SLP	τ_x	τ_y	NINO 3.4	<i>R</i>	obs	σ model	
Cres City	1.61	-0.02	0.04	3.61	0.82	17.2	14.2	0.66
San Fran	1.37	0.01	0.04	5.33	0.79	12.3	9.7	0.75
La Jolla	1.15	-0.03	0.02	5.49	0.67	8.6	5.7	0.85

^a τ_x and τ_y are west-to-east and south-to-north wind stress components, respectively.

^b Correlation between seasonal (Nov–Mar) non-tide residuals and ENSO index from NINO 3.4 SSTs.

Table 4 Modeled San Francisco Sea Level exceedances occurring with prescribed mean sea level trend

GFDL A2 Trend cm/ 100 year	Number of exceedances		
	2005–2034 99.99%	2035–2064 99.99%	2070–2099 99.99%
0	15	27	23
10	19	61	57
20	24	112	156
30	39	205	529
40	63	380	1,470
50	97	679	3,553
60	139	1,238	7,072
70	209	2,152	12,674
80	306	3,455	20,232

99.99% threshold 141 cm is from observed 1960 to 1978 hourly data at San Francisco. Trends are linear from 2000 to 2100 weather and ENSO impact in sea level simulations from the GFDL CM2.1 A2 emissions scenario.

occurrence of extremes with hypothetical sea level rise are found in the modeled sea levels at La Jolla and Crescent City (not shown).

The influence of weather events and ENSO in producing high sea level extremes is evidenced by two additional runs of the statistical model, one with no weather and one with no weather and no ENSO input, shown in Table 5. The “no weather, no ENSO” simulations indicate that these natural fluctuations are required to produce virtually all of the hourly sea level exceedances above the historical (1960–1978) 99.99 percentile threshold. When the largest (80 cm/century) SLR rates are imposed and as time progresses, these exceedances become more and more prevalent, until, with the largest trends during the 2070–2099 period, the number of exceedances from “no weather, no ENSO” reach almost the same level as those produced by the “full” model of weather, ENSO, tide and trend components. The “no weather” simulations indicate that synoptic scale (a few days) weather disturbances play a critical role in generating extremes, with more than half of the 99.99 percentile level exceedances during the historical period eliminated during the “no weather” run. On the other hand, these results also illustrate the key role played by ENSO in producing sea level extremes, as the exceedances that remain can be attributed to ENSO effects.

Considering the ranges of SLR expected from the three emissions scenarios (Fig. 3), if warming is modest so that SLR rates are at the low end of the projected envelope, the increases in extreme events would increase, but not greatly; in this case, temperatures, SLR

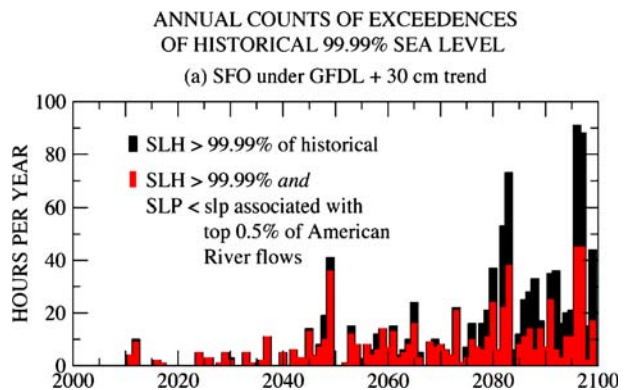
Table 5 Number of occurrences of hourly sea level events above historical 99.99 percentile at San Francisco, where sea level is rising at 30 cm/century, with: (a) tides, trend, weather and ENSO; (b) tides, trend, ENSO; and (c) tides and trend

GFDL A2 30 cm trend	2005–2034	2035–2064	2070–2099
Model components			
Tides, trend, weather, ENSO	39	205	529
Tides, trend, ENSO	1	6	251
Tides, trend	0	1	142

and sea-level extremes from the three scenarios (B1, A2, A1fi) would not be that different from each other. On the other hand, if warming is large so as to push SLR towards higher end of the projected envelope, the incidence of extreme events would increase markedly and the three scenarios (B1, A2, A1fi) would be sharply differentiated. In this case, the highest emission scenario would produce a much greater occurrence of high sea level events.

In addition to its effects on the open coast, SLR and attendant inundations may have severe impacts on low-lying land bordering the San Francisco Bay and Delta. This would damage marginal ecosystems as well as degrading the quality and reliability of the fresh water supply pumped from the southern edge of the San Francisco Delta. Inundation would be worsened when high sea levels are exacerbated by freshwater floods. To explore this, Fig. 6 shows – for the San Francisco (SFO) sea-level scenario based on the GFDL climate under A2 emissions and with an assumed sea-level trend of 30 cm/century – the counts of hours per year with SFO sea levels above the 99.99% historical sea-level range (in black). Also shown are corresponding counts of high sea-level stands that co-occurred when the simulated SFO sea-level pressure (SLP) was low enough to produce stormy and wet weather. To estimate this SLP threshold, daily SLPs were regressed against daily flows in the North Fork American River during November–March from 1949 to 1999 to quantify how SLP levels correspond to various flow levels in central Sierra Nevada Rivers. The 90 historical days with largest flows in the North Fork American River (average of 2/year, top 0.5% of observed flows) were identified, and from those flows, a historical 99.5% exceedance level for flows in the American River was estimated. The SLP threshold corresponding to that flow threshold was then estimated from the flow-SLP regression equation (-4 mb). Using this SLP threshold, the number of hours per year during which both (a) sea levels exceeded the 99.99% threshold and (b) the SLP values were lower than the SLP threshold were plotted (Fig. 6, in red). The sequences shown indicate that, under the 30 cm/century SLR rate, the storm/high-sea level coincidences increases at least until about mid-century and, indeed, makes up most of the increasing numbers of sea-level threshold exceedances until then. Sometime near mid-century, the number of coincidences saturates (becomes more or less stable but still much more common than in the historical period or early decades of the twenty-first century) and the total number of sea-level exceedances, not associated with low SLPs, continues to grow. As indicated earlier, synoptic scale weather disturbances are critical contributors to the observed and projected sea-level extremes, at least until SLR has markedly raised the base levels from which other influences generate extremes. In the Bay and Bay-ward parts of the Delta, this sequence of

Fig. 6 Projected total exceedances of San Francisco hourly sea level height (SLH) above historical 99.99 percentile (*black*), and the number that are coincident with sea level pressure anomalies less than -4 mb (*red*). Projected sea level from GFDL model weather and NINO 3.4 SST with a linear trend of 30 cm over 2000–2100



new sea-level exceedances suggest that the number of opportunities for high-sea-level stands and floods to coincide may increase most rapidly in the early-to-middle stages of twenty-first century sea-level rise.

6 Waves and sea level

Most coastal damage in California occurs during periods when both extreme sea levels and extreme wave heights occur concurrently (Flick 1998). The additional impact that waves may add to high coastal sea levels can be characterized probabilistically, recognizing that wave amplitudes are related to storminess, which is related to sea level anomalies. In the PCM and GFDL model projections employed here, storminess along the California coast is marked by interannual and decadal variability, similar to the last several decades of various instrumental records (Bromirski et al. 2003 and Fig. 7, lower), but shows little tendency for a secular change over the twenty-first century, as shown by the incidence of low sea level pressure events plotted in Fig. 7, upper. The relationship between significant wave height (H_s ; the average height of the highest one-third waves) and non-tidal sea levels can be described using historical wave buoy and sea level records in Northern California (near Crescent City), Central California (near San Francisco), and Southern California (near La Jolla), from approximately 1981–present. Extreme wave heights and extreme non-tide sea level fluctuations tend to increase from the south to the north along the California coast, demonstrated by Gaussian probability distributions of the ranked estimates (Fig. 8). The most dramatic change, moving northward along the coast, is the large increase in wave heights (Fig. 8, right) between Pt. Conception (SCA, green) and San Diego (SIO, blue), with San Diego shielded – along with the rest of the Southern California Bite coastline – by Pt. Conception and the Channel Islands. Differences in the wave energy probability distributions between Pt. Conception and locations farther north, near San Francisco (CCA) and Crescent City (NCA), are small, except only for the most extreme waves. The similarity of wave heights north of Pt. Conception reflects the fact that, to the north, a dominant mode of wave height variability is shared all along the central and northern California coasts (Bromirski et al. 2005).

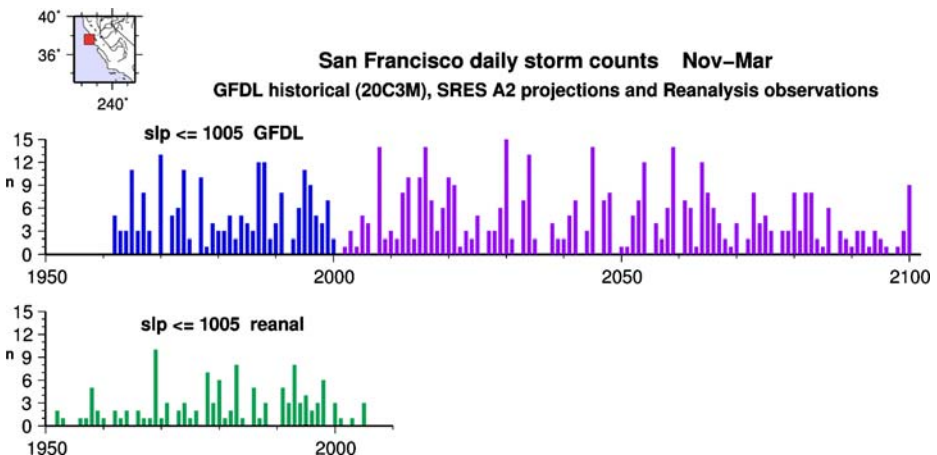


Fig. 7 Number of days per year of events when SLP is 1005 hPa or lower in vicinity of San Francisco from GFDL A2 simulation 1962–2100 (*upper*), and from NCEP/NCAR Reanalysis 1950–2004 (*lower*)

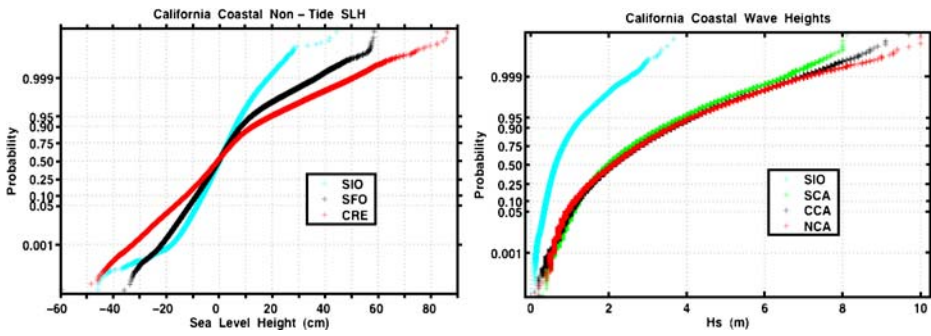


Fig. 8 (left) Normal (Gaussian) probability distributions for hourly non-tide sea levels at La Jolla (SIO), San Francisco (SFO), and Crescent City (CRE). (right) Normal (Gaussian) cumulative probability distributions for hourly significant wave height near San Diego (SIO), Pt. Conception (SCA), San Francisco (CCA), and Crescent City (NCA)

Extreme sea level height fluctuations are also larger to the north, as a result of increasing storm intensities at the more northerly coastal locations (Fig. 8, left). The non-tide sea levels are obtained by spectrally removing the tidal energy from the hourly tide gauge records (Bromirski et al. 2003). Note that, for example, a 30 cm event is much less likely near San Diego (SIO) than near either San Francisco (SFO) or Crescent City (CRE).

The probabilities of the potentially important co-occurrences of extreme waves and extreme sea level heights are illustrated for peak H_s 's at NOAA buoys near San Francisco in Fig. 9. The probability distribution in Fig. 9 shows the historical (1981–present)

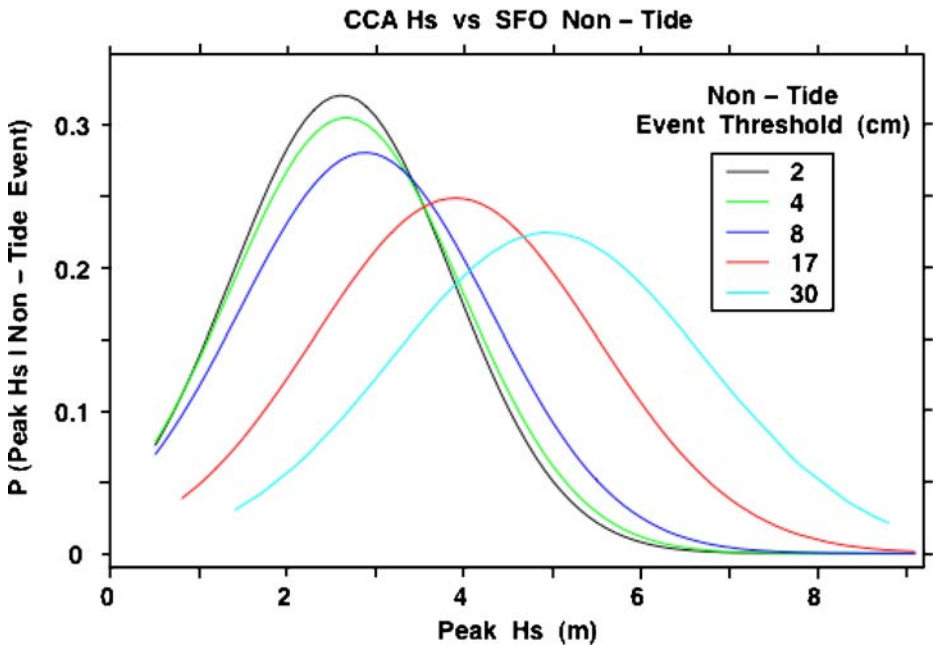


Fig. 9 Association of significant wave heights (H_s) at central California coastal buoys with non-tidal sea level anomalies at San Francisco. Each curve represents the conditional probability of H_s during a storm event characterized by non-tidal levels exceeding selected thresholds

frequencies of occurrences of peak Hs's during times when the non-tide sea level heights were continuously above the 25th, 50th, 75th, 95th, and 99th percentile thresholds for at least 3 h, respectively. The resulting distributions indicate that higher Hs's are more likely during higher anomalous non-tide sea-level stands than during lower sea-level anomalies. For example, the most likely value of peak Hs rises from about 2.5 to over 5 m, as non-tide sea level anomalies increase from 4 to 30 cm. This reflects the important role of storms in driving, often simultaneously, high sea levels and high waves.

7 Summary

Coastal observations and global climate projections indicate that California's coast will be affected by sea level rise (SLR) during the twenty-first century. There is much uncertainty in global SLR projections, so the present analysis explores a range of outcomes – this is a scenarios analysis, not a prediction. SLR projected using output from recent global climate model runs increases in proportion to the amount of global warming. By 2070–2099, projected SLR ranges from 13 to 76 cm, depending on the magnitude of climate warming (which is generally larger for scenarios with higher projected greenhouse gas concentrations). The middle to higher end of this range would substantially exceed the historical rate of sea level rise, approximately 20 cm/century, observed at San Francisco and San Diego during the past 100 years.

Problems created by SLR are greatly aggravated by higher frequency sea level phenomena. In particular, sea-level extremes are even more dangerous in many settings than are the long-term mean rises themselves, and the extremes occur when the long-term changes coincide with shorter period fluctuations. These other higher frequency fluctuations derive from tides, weather, and climatic fluctuations such as El Niño/Southern Oscillation events. The present study considers output from two climate models (GFDL and PCM) and three emission scenarios to provide a set of future weather and short period climate fluctuations, and a range of potential long-term sea level rises. Using a model of the combined contributions to hourly sea level of predicted tides and model-simulated weather, climate, and long-term global warming, the potential for SLR-induced changes in the occurrence of hourly extremes was assessed. If sea level rise trends are near the low end, the occurrence of extremely high-sea level events will increase, but the increase in extremes would be not so different from the increase in extremes that has been experienced along the California coast during the last several decades, as outlined in Table 1. On the other hand, if sea level rises climb to the higher end, extreme events and their duration would increase markedly, substantially beyond any recent increase during California's nineteenth and twentieth century human experience.

Coastal sea level extremes are also exacerbated by other storm effects, such as heavy surf from wind-driven waves. Implications are that when short term anomalous sea level is highest, wave energy has an increased likelihood of reaching very high levels. When these factors coincide with high tides, the chances for coastal damage are greatly heightened. Continuing increases in mean sea level due to global change makes this problem ever more severe.

In the San Francisco Bay estuary, sea level rise effects may be compounded by riverine floods that feed into the northern reaches of the Bay from the Sacramento/San Joaquin Delta. Storms are important causes of the highest water levels both because of the barometric and wind effects on the sea levels that accompany them, and because of the (freshwater) floods that they can generate. As climate warms, snow levels rise, and

snowmelt comes faster, the Sierra Nevada watershed would generate rapid (storm-time) runoff over a larger range of elevations. The combination of flooding and high sea-level stands is particularly dangerous in the Delta, where the combination of sea level and river stages determine water heights.

Acknowledgments Comments by David Jay, Douglas Inman and two anonymous reviewers were very helpful. Thanks to Martha Coakley for data processing and analyses. Funding for PB and DC was provided by the California Department of Boating and Waterways and for CH, PB, MT and DC by the California Energy Commission PIER Program. MD and DC were also supported by the USGS Priority Ecosystems Study and MT, MD and MT by the NOAA RISA Program.

References

- Alley RB, Clark PU, Huybrechts P, Joughin I (2005) Ice-sheet and sea-level changes. *Science* 310:456–460
- Bromirski PD, Flick RE, Cayan DR (2003) Decadal storminess variability along the California coast: 1858–2000. *J Clim* 16:982–993
- Bromirski PD, Cayan DR, Flick RE (2005) Wave spectral energy variability in the northeast Pacific. *J Geophys Res* 110:C03005, DOI [10.1029/2004JC002398](https://doi.org/10.1029/2004JC002398)
- Cabanes C, Cazenave A, Le Provost C (2001) Sea level rise during the past 40 years determined from satellite and in situ observations. *Science* 294:840–842
- Cazenave A, Nerem RS (2004) Present-day sea level change: observations and causes. *Rev Geophys* 42:RG3001, DOI [10.1029/2003RG000139](https://doi.org/10.1029/2003RG000139)
- Chelton DB, Davis RE (1982) Monthly mean sea-level variability along the west coast of North America. *J Phys Oceanogr* 12:757–784
- Church JA, White NJ (2006) twentieth century acceleration in sea level rise. *Geophys Res Lett* 33: (L01602) DOI [10.1029/2005GL024826](https://doi.org/10.1029/2005GL024826)
- Church JA, Gregory JM, Huybrechts P, Kuhn M, Lambeck K, Nhuan MT, Qin D, Woodworth PL (2001) Changes in sea level. Chapter 11 of the intergovernmental panel on climate change third assessment report. Cambridge University Press, Cambridge, pp pp 639–694
- Delworth T et al (2006) GFDL's CM2 global coupled climate models – Part 1: formulation and simulation characteristics. *J Clim* 19(5):643–674
- Fairbanks RG (1989) A 17,000-year glacio-eustatic sea level record: influence of glacial melting rates on the Younger Dryas event and deep-ocean circulation. *Nature* 342(6250):637–642
- Flick RE (1998) Comparison of California tides, storm surges, and mean sea level during the El Niño winters of 1982–1983 and 1997–1998. *Shore & Beach* 66(3):7–11
- Flick RE (2000) Time-of-day of peak tides in a mixed-tide regime. *Shore & Beach* 68(4):15–17
- Flick RE, Murray JF, Ewing LC (2003) Trends in United States tidal datum statistics and tide range. *J. Waterway, Port, Coastal and Ocean Eng.*, Amer Soc Civil Eng 129(4):155–164
- Gregory JM, Church JA, Boer GJ, Dixon KW, Flato GM, Jackett DR, Lowe JA, O, Farrell SP, Roeckner E, Russell GL, Stouffer RJ, Winton M (2001) Comparison of results from several AOGCMs for global and regional sea-level change 1900–2100. *Clim Dyn* 18:225–240
- Hansen J (2005) Earth's energy imbalance: confirmation and implications. *Science* 308(5727):1431–1435
- Holgate SJ, Woodworth PL (2004) Evidence for enhanced coastal sea level rise during the 1990's. *Geophys Res Lett* 31: L07305, DOI [10.1029/2004GL019626](https://doi.org/10.1029/2004GL019626)
- Hulme M, Raper SCB, Wigley TML (1995) An integrated framework to address climate change (ESCAPE) and further developments of the global and regional climate modules (MAGICC). *Energy Policy* 23:347–355
- Kalnay E, Kanamitsu M, Kistler R, Collins W, Deaven D, Gandin L, Iredell M, Saha S, White G, Woollen J, Zhu Y, Leetmaa A, Reynolds B, Chelliah M, Ebisuzaki W, Higgins W, Janowiak J, Mo KC, Ropelewski C, Wang J, Jenne R, Joseph D (1996) The NCEP/NCAR 40-year reanalysis project. *Bull Amer Meteor Soc* 77:437–471
- Meehl GA et al (2005) How much more global warming and sea level rise? *Science* 307(5716):1769–1772
- Mitrovica JX, Tamisiea ME, Davis JL, Milne GA (2001) Recent mass balance of polar ice sheets inferred from patterns of global sea level change. *Nature* 409:1026–1029
- Mitrovica JX, Wahr J, Matsuyama I, Paulson A, Tamisiea ME (2006) Reanalysis of ancient eclipse, astronomic and geodetic data: a possible route to resolving the enigma of global sea-level rise. *Earth and Planetary Sci Lett* 243:390–399

- Munk WH (2002) Twentieth century sea level: an enigma. *Proc Nat Acad Sci* 99(10):6550–6555
- Munk WH, Cartwright DE (1966) Tidal spectroscopy and prediction. *Phil Trans Roy Soc London* 259:533–581
- Ryan H, Gibbons H, Hendley JW, Stauffer P (2000) El Niño sea-level rise wreaks havoc in California's San Francisco Bay Region. USGS Fact Sheet 175–99. Available online at: <http://geopubs.wr.usgs.gov/fact-sheet/fs175-99/>
- Seymour RJ (1998) Effects of El Niños on the west coast wave climate. *Shore and Beach* 66(3):3–6
- Seymour RJ, Strange RR, Cayan DR, Nathan RA (1984) Influence of El Niños on California's wave climate: *in* Proceedings of the 19th Coastal Engineering Conference: American Society of Civil Engineers. v. 1, p. 577–592
- Storlazzi CD, Griggs GB (1998) The 1997–98 El Niño and erosion processes along the central coast of California. *Shore and Beach* 66(3):12–17
- Trenberth K, Hurrell J (1994) Decadal atmosphere–ocean variations in the Pacific. *Climate Dynamics* 9:303–319
- Wallace JM, Gutzler DS (1981) Teleconnections in the geopotential height field during the Northern-Hemisphere winter. *Mon Wea Rev* 109:784–812
- Washington WM, Weatherly JW, Meehl GA, Semtner AJ, Bettge TW, Craig AP, Strand WG, Arblaster J, Wayland VB, James R, Zhang Y (2000) Parallel Climate Model (PCM) control and transient simulations'. *Clim Dyn* 16(10/11):755–774
- White NJ, Church JA, Gregory JM (2005) Coastal and global averaged sea level rise for 1950 to 2000. *Geophys Res Lett* 32: L01601, DOI 10.1029/2004GL021391
- Wigley TML (2005) The climate change commitment. *Science* 307:1766–1769
- Zetler DB, Flick RE (1985) Predicted extreme high tides for mixed tidal regimes. *J Phys Oceanogr* 15 (3):357–359